Drawbacks of applying perturbative schemes to meson spectroscopy *)

K. P. KHEMCHANDANI[1,**], Eef van BEVEREN[1], George RUPP[2]

[1] *Centro de Física Computacional, Departamento de Física, Universidade de Coimbra, P-3004-516 Coimbra, Portugal*

[2] *Centro de Física das Interacções Fundamentais, Instituto Superior Técnico, Universidade Técnica de Lisboa, P-1049-001 Lisboa, Portugal*

We study meson-meson scattering in a soluble model which describes asymptotically free mesons and confined quark-antiquark pairs via coupled channels. Concretely, the two scattered mesons are assumed to interact through s-channel meson-exchange diagrams. Furthermore, we develop a perturbative expansion of the model, and show that the thus found resonance pole positions, including contributions up to fourth order in perturbation theory, completely fail to reproduce the exact results. This shows that the resonance predictions based on perturbative approximations in quark models may be highly unreliable.

§1. Introduction

Hadron spectroscopy in present times appears to have become subdivided into many different fields of interest, like conventional quark spectroscopy, hadronic molecular states, dynamically generated resonances, tetraquarks and pentaquarks, glueballs, gluonic hybrids, and so forth. The advancement of detector and analysis techniques at the many new experimental facilities in the intermediate-energy range has been resulting in the observation of more and more hadronic states, many of which no not seem to fit into the traditional quark spectrum of $q\bar{q}$ mesons and qqq baryons. This has led to the investigation of other possible configurations that might be viable within QCD. On the one hand, this makes it important and interesting to explore the structure and properties of hadrons, which may shed light on the dynamics of strong interactions at low energies. On the other hand, though, a very careful analysis is required, in order to avoid confusions and controversies. We are convinced that the most important need of present-day research in hadron spectroscopy is some consensus on the ideal quark model to confront with the data. And right now is probably the best moment to tackle this problem, since quite a lot of data, at least concerning meson spectroscopy, is being produced (see for example Refs.[1),2),3),4),5),6),7),8),9)]), and even more data, of better quality, is expected in the near future. All this could help gather a vastly improved understanding of quarkonia and other mesonic resonances. However, in such a situation it is extremely important to first agree on the hadron spectrum, as obtained from a chosen quark model,

*) Based on notes for a talk presented by Eef van Beveren at the *11th International Conference on Meson-Nucleon Physics and the Structure of the Nucleon*, September 10-14 (2007) IKP Forschungzentrum Jülich (Germany).

**) Present address: Research Center for Nuclear Physics (RCNP), Ibaraki, Osaka 567-0047, Japan.

since only then valid conclusions can be drawn about possible incompatibilites with standard quark configurations.

Indeed a lot of work is being done on trying to understand the conventional and unconventional structure of different "exotic" hadrons. For example, a very interesting analysis of the quark content and possible molecular nature of many newly found mesonic states has been carried out on the basis of QCD sum rules,[10),11)] while an attempt to distinguish between quarkonium and hybrid states was made in Ref.[12)] Another very interesting investigation, namely of the quark and molecular content of baryon resonances, was reported in Ref.[13)] Furthermore, Ref.[14)] nicely explained the phenomenon of dynamically generated resonances and the concept of dynamical reconstruction, in order to be able to pinpoint (dominantly) $q\bar{q}$ states. All these meticulous efforts and the corresponding results would get more merit, if a universally agreed conventional hadron spectrum was known.

The main issue is that experimental evidence for possible resonances is obtained from total or partial-wave cross sections, as well as angular distributions and decay modes. In order to interpret the data, one needs a model, since perturbative QCD cannot be used at low energies. In the present paper, we will focus on non-exotic meson-meson scattering. Nevertheless, the results can easily be generalized for application to hadron-pair production.[15)] We intend to describe the cross sections and resonance pole positions for meson-meson scattering in an as large as possible energy range, rather than focusing on just one peak. At this point enters the main philosophy behind the model, namely that the enhancement structure of cross sections in non-exotic meson-meson scattering stems from the quark-antiquark spectrum. Consequently, for such reactions we must study a coupled system of a $q\bar{q}$ state and non-exotic two-meson channels. This is an absolutely minimal requirement for modeling the cross sections in this case. Further extensions to multiquark or hybrid resonances might be contemplated in case the minimal model turns out not to reproduce the experimental data sufficiently well. Furthermore, the proposed strategy[16),17)] simultaneously covers two-meson molecules and $q\bar{q}$ systems. Hence, the physical solutions are not just pure $q\bar{q}$ or molecular states, but rather mixtures of these two configurations. One could then try to find out which component is dominant.[18),19),20)] However, that lies beyond the scope of this paper. In more popular terms, one might refer to the states obtained from such a model as $q\bar{q}$ systems surrounded by a meson cloud. In the past, our approach was also called the unitarization scheme for the quark-antiquark system.[21),22),23),24)]

The model we are going to use treats confined quarks and hadronic decay channels on an equal footing, via coupled channels, regardless of whether the energy is above or below the thresholds of the decay channels. It was developed in Refs.,[16),17),25),26),27)] and has been extensively used to study the properties of mesonic resonances (for some of the recent works, see Refs.[28),29),30),31),32),33)] and references therein). The effective meson-meson potential in the model consists of s-channel exchange of a confined $q\bar{q}$ pair, with radial quantum number running from 0 to infinity and orbital angular momentum compatible with total J^{PC}. The importance of hadron dynamics in understanding the meson spectrum for low and intermediate energies already becomes obvious from the fact that it easily gets en-

ergetically favorable for the "string" between the quark and the antiquark to break, alongside the creation of a new and light $q\bar{q}$ pair, which then may lead to hadronic decay. An even stronger indication comes from the light scalar mesons, whose unconventional nature is related to their very strong coupling to S-wave two-meson channels.[34] The latter work also shows that the inclusion of bare-meson exchange in the s-channel, in addition to the meson-meson contact interaction,[23),35),36),37),38)] in certain cases leads to finding new states which might be absent when considering contact interactions only. This phenomenon was explained very neatly in Ref.,[27)] where it was shown that, for the study of a restricted energy range corresponding to a particular resonance, the contribution from different diagrams involving meson exchange with different quantum numbers gives rise to a constant interaction, which is equivalent to considering a contact interaction in unitarized models. It was further shown in Ref.[27)] that, in order to understand a larger energy range, covering several resonances, meson-exchange diagrams are required as well. This explains why the common use of contact interactions in unitarized models, to study dynamically generated hadron resonances, works quite well.[39),40),41),42),43),44),45),46),47)] However, from Ref.[27)] it becomes clear that the development of a broader and more general perspective for hadron spectroscopy requires the treatment of quarks and hadrons as coupled systems. In this paper, we will show that not only the handling of coupled mesons and quarks is necessary, but also the full solution of the scattering equations is essential. In particular, we will demonstrate that approximating resonance pole positions perturbatively leads to unreliable results.

In the next section, we will first describe the exact formalism, followed by the construction of a perturbative expansion thereof. In the subsequent sections, we will choose some specific examples to show that no meaningful results can be obtained from the perturbative expansion. Finally, we will summarize the detailed discussions in the paper.

§2. Formalism

We study meson-meson scattering using a model in which quarks and hadrons are considered coupled systems. The formalism amounts to solving a scattering equation for mesons, with the lowest-order term of the Born series given by an effective interaction due to the exchange of a confined $q\bar{q}$ pair. The potential between the latter pair is written in terms of a harmonic oscillator. The eigenenergies of the harmonic oscillator thus correspond to the bare $q\bar{q}$ spectrum. The effective meson-meson potential, which is the lowest-order term of the full scattering amplitude, involves an infinite sum over all the diagrams with s-channel $q\bar{q}$ exchange, having different radial quantum number n ($0 \leq n < \infty$), as shown in Fig. 1 below.

Although not strictly necessary, it is illustrative to consider a formulation of the model in terms of a coupled system of nonrelativistic Hamiltonians. However, a rigorous derivation in terms of a sum of meson loops, which leads to the same final result, is also possible.

Since the model is based on coupling a confined quark-antiquark pair and a

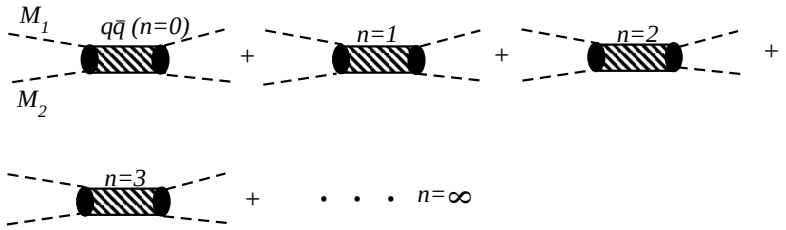

Fig. 1. The meson-meson potential, i.e., the Born term of the full scattering amplitude, which involves the exchange of a confined $q\bar{q}$ pair, with radial quantum number n running from 0 to ∞.

meson pair, we describe the system by the equations

$$H_c\psi_c(\vec{r}) + V_T(\vec{r})\psi_f(\vec{r}) = E\psi_c(\vec{r}), \tag{2·1}$$
$$H_f\psi_f(\vec{r}) + V_T(\vec{r})\psi_c(\vec{r}) = E\psi_f(\vec{r}), \tag{2·2}$$

where the subscripts "c" and "f" (here and throughout this article) refer to the confined quarks and free mesons (i.e., considering them plane waves), respectively, and V_T is the transition potential between the two sectors.

H_c and H_f describe the Hamiltonians of these sectors, reading

$$H_c = -\frac{\nabla_r^2}{2\mu_c} + m_q + m_{\bar{q}} + V_c(r), \tag{2·3}$$
$$H_f = -\frac{\nabla_r^2}{2\mu_f} + M_1 + M_2, \tag{2·4}$$

where the confining potential is assumed to be a harmonic oscillator, viz.

$$V_c = \frac{1}{2}\mu_c\omega^2 r^2, \tag{2·5}$$

with μ_c and ω the reduced mass and frequency of the $q\bar{q}$ system, respectively. Furthermore, M_1, M_2, and m_q, $m_{\bar{q}}$ are the meson and quark masses, respectively. Our choice of a harmonic-oscillator potential in the confined sector is based on earlier observations of regular spacings in the quarkonium spectra,[16),17)] which seem to be confirmed by states found in even the most recent experiments.[28),48),49),50)] In writing down the equations above, we have assumed only one $q\bar{q}$ and one meson-meson channel, for the sake of simplicity. These equations can be straighforwardly generalized to the multichannel case, taking then a matrix form.[31)]

Now, Eqs. (2·2) and (2·1) can be rewritten as

$$(E - H_c)\psi_c(\vec{r}) = V_T(\vec{r})\psi_f(\vec{r}), \tag{2·6}$$
$$(E - H_f)\psi_f(\vec{r}) = V_T(\vec{r})\psi_c(\vec{r}).$$

Then, the confinement wave function $\psi_c(\vec{r})$ must be eliminated from the equations, as it never develops into an asymptotic state. Thus we get

$$\psi_f(\vec{r}) = (E - H_f)^{-1}V_T(E - H_c)^{-1}V_T\psi_f(\vec{r}). \tag{2·7}$$

From first principles of standard scattering theory, we can conclude that the factor

$$V_T(E - H_c)^{-1}V_T \tag{2·8}$$

acts like an "effective" meson-meson potential, which, if denoted by V_{MM}, implies

$$\langle \vec{P}_f \mid V_{MM} \mid \vec{P}'_f \rangle = \langle \vec{P}_f \mid V_T(E(\vec{P}_f) - H_c)^{-1}V_T \mid \vec{P}'_f \rangle, \tag{2·9}$$

where the total center-of-mass energy (CM) E is given by

$$E(p_f) = \frac{(\vec{P}_f)^2}{2\mu_f} + M_1 + M_2, \tag{2·10}$$

with μ_f the reduced mass of the two mesons, and P_f (P'_f) denoting the CM momentum of the two-meson initial (final) state.

Furthermore, we denote the energy eigenvalue of H_c by E_{nl}, i.e.,

$$E_{nl} = \omega(n_c + l_c + 3/2) + M_q + M_{\bar{q}}, \tag{2·11}$$

and the corresponding eigensolutions by $\langle \vec{r}_c \mid n_c, l_c, m_c \rangle$. By introducing in Eq. (2·9) a complete set corresponding to this state, we get

$$\begin{aligned}
&\langle \vec{P}_f \mid V_{MM} \mid \vec{P}'_f \rangle \\
&= \sum_{n_c,l_c,m_c} \langle \vec{P}_f \mid V_T \mid n_c, l_c, m_c \rangle \langle n_c, l_c, m_c \mid (E(\vec{P}_f) - H_c)^{-1} V_T \mid \vec{P}'_f \rangle \\
&= \sum_{n_c,l_c,m_c} \langle \vec{P}_f \mid V_T \frac{\mid n_c, l_c, m_c \rangle \langle n_c, l_c, m_c \mid}{(E(\vec{P}_f) - E_{nl})} V_T \mid \vec{P}'_f \rangle,
\end{aligned} \tag{2·12}$$

which, upon further introduction of several complete sets corresponding to the meson-meson configuration space, gives

$$\begin{aligned}
\langle \vec{P}_f \mid V_{MM} \mid \vec{P}'_f \rangle \; = \; & \sum_{n_c,l_c,m_c} \int d^3 r_f \int d^3 r'_f \int d^3 r''_f \int d^3 r'''_f \frac{\langle \vec{P}_f \mid \vec{r}_f \rangle}{(E(\vec{P}_f) - E_{nl})} \times \\
\times \langle \vec{r}_f \mid V_T \mid \vec{r}''_f \rangle \langle \vec{r}''_f \mid n_c, l_c, m_c \rangle & \langle n_c, l_c, m_c \mid \vec{r}'''_f \rangle \langle \vec{r}'''_f \mid V_T \mid \vec{r}'_f \rangle \langle \vec{r}'_f \mid \vec{P}'_f \rangle.
\end{aligned} \tag{2·13}$$

For the transition potential, we take a local delta-shell function of the form

$$\langle \vec{r}_f \mid V_T \mid \vec{r}'_f \rangle = \frac{\lambda}{\mu_c a} \delta(r_f - a) \delta^3(\vec{r}_f - \vec{r}'_f). \tag{2·14}$$

This form of potential has been proven useful in describing the breaking of the color string.[51] The λ and a in Eq. (2·14) are the two parameters of the model, with the former being the coupling of the meson channel to the quark channel, and the latter an average distance between the quarks. The coupling λ is varied between 0 and 1 in the present study, with $\lambda = 0$ corresponding to decoupled meson and quark systems. Since the meson-meson state is considered a plane wave, decoupling would result in a pure ("bare") $q\bar{q}$ spectrum. On the other hand, $\lambda \geq 1$ represents strong coupling to the meson-meson channel. The parameter a is taken in the range 3–5 fm.

Using the above form for V_T, and the normalization $\langle \vec{r} \mid \vec{p} \rangle = e^{i\vec{p}\cdot\vec{r}}/(2\pi)^{3/2}$, Eq. (2·13) becomes

$$\langle \vec{P}_f \mid V_{MM} \mid \vec{P}'_f \rangle = \sum_{n_c,l_c,m_c} \int \frac{d^3r_f}{\sqrt{(2\pi)^3}} \int \frac{d^3r'_f}{\sqrt{(2\pi)^3}} e^{-i\vec{P}_f\cdot\vec{r}_f} \frac{\lambda}{\mu_c a} \delta(r_f - a) \times$$
$$\times \frac{\langle \vec{r}_f \mid n_c, l_c, m_c \rangle \langle n_c, l_c, m_c \mid \vec{r}'_f \rangle}{E(\vec{P}_f) - E_{nl}} \frac{\lambda}{\mu_c a} \delta(r'_f - a) e^{i\vec{P}'_f\cdot\vec{r}'_f}. \qquad (2\cdot15)$$

The functions $\langle \vec{r_f} \mid n_c, l_c, m_c \rangle = Y^{l_f}_{m_f}(\hat{r}) \langle |\vec{r_f}| \mid n_c, l_c, m_c \rangle$ represent an overlap wave function of the meson-meson $\to q\bar{q}$ vertex. In order to determine this overlap function, we assume a mechanism for the transition from the meson channel to the quark channel, or vice versa. To describe this mechanism, let us consider a confined quark-antiquark pair with total spin, angular momentum, intrinsic spin, and radial quantum number j, l_1, s_1, and n_1, respectively. As one usually expects from QCD at low Q^2, it is assumed that the string between the quark and the antiquark breaks with the creation of a new $q\bar{q}$ pair. This new pair is assumed to have vaccuum quantum number, corresponding to a $^{2s_2+1}l_{2\,j_2} = {}^3P_0$ state. This yields two $q\bar{q}$ pairs, which then rearrange to produce two mesons with quantum numbers j'_1, l'_1, S'_1, n'_1 and j'_2, l'_2, S'_2, n'_2, respectively (see Fig. 2).

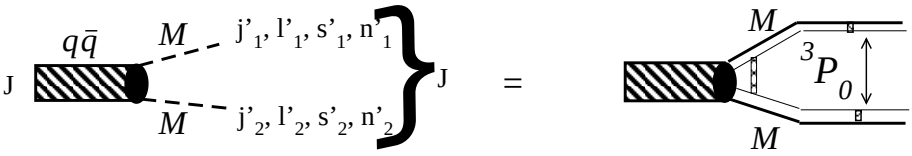

Fig. 2. The transition vertex from the quark channel to the two-meson channel.

Mathematically, the rearrangement of the two $q\bar{q}$ pairs, one of which is a $^3P_0$ state and the other having the quantum numbers of the decaying meson, can be expressed by treating them as four independent nonrelativistic harmonic oscillators. Let us label them with numbers, and assume that system (1+2) represents the quark-antiquark pair under consideration, while system (3+4) stands for the newly created $^3P_0$ $q\bar{q}$ pair. This can be treated as a four-body problem, which can be reduced to a three-body problem in the global CM system, by considering the coordinates (momenta) of the CM of the $(1+2)$, $\vec{r}_{12}(\vec{p}_{12})$, and $(3+4)$, $\vec{r}_{34}(\vec{p}_{34})$ systems, along with their relative motion $\vec{r}_{1234}(\vec{p}_{1234})$. The situation after the transition is described by assuming that the $(1+4)$ and $(3+2)$ systems represent the two meson state. This can be represented diagrammatically, as shown in Fig. 3.

The Hamiltonians for the systems, before and after the transition, can be written in the global CM frame as

$$H_{\rm before} = \frac{1}{2}\omega\Big\{r^2_{12} + r^2_{34} + r^2_{1234} + p^2_{12} + p^2_{34} + p^2_{1234}\Big\}, \qquad (2\cdot16)$$

$$H_{\rm after} = \frac{1}{2}\omega\Big\{r^2_{14} + r^2_{32} + r^2_{1432} + p^2_{14} + p^2_{32} + p^2_{1432}\Big\}, \qquad (2\cdot17)$$

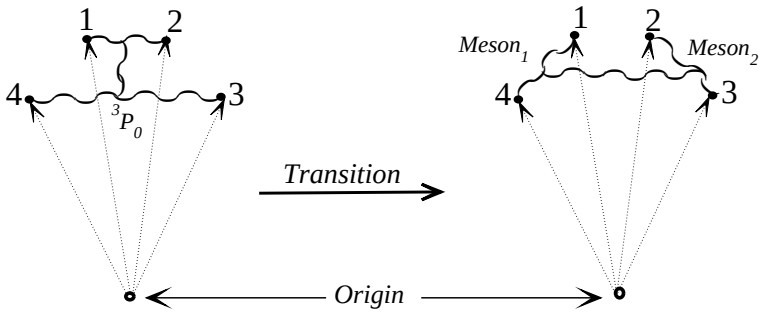

Fig. 3. The four quarks, labeled by numbers, before and after the transition. It is assumed that before the transition the string between a $q\bar{q}$ pair (1 and 2) breaks to form a new pair (3 and 4), with $^3P_0$ quantum numbers, and the whole system rearranges so as to produce two mesons made of the quark pairs 1-4 and 3-2.

where r_{ij} (p_{ij}) is the coordinate (momentum) of the ij system, and r_{ijkl} (p_{ijkl}) is the relative coordinate (momentum) of the CM of the ij and kl systems. The transition of e.g. the coordinates of the four quarks can be expressed in terms of an orthogonal transformation matrix α (as explained in Ref.[25]), i.e.,

$$\begin{pmatrix} r_{14} \\ r_{32} \\ r_{1432} \end{pmatrix} = \begin{pmatrix} \alpha_{11} & \alpha_{12} & \alpha_{13} \\ \alpha_{21} & \alpha_{22} & \alpha_{23} \\ \alpha_{31} & \alpha_{32} & \alpha_{33} \end{pmatrix} \begin{pmatrix} r_{12} \\ r_{34} \\ r_{1234} \end{pmatrix} . \tag{2·18}$$

Thus, if the wave functions of the systems before and after the transition are written as $\psi^E_{\{n,l,m\}}(r_{12}, r_{34}, r_{1234})$ and $\chi^E_{\{n',l',m'\}}(r_{14}, r_{32}, r_{1432})$, respectively, then

$$\langle \psi^E_{\{n,l,m\}}(r_{12}, r_{34}, r_{1234}) | = \sum_{n',l',m'} \int dr_{14} \int dr_{23} \int dr_{1234}$$
$$\langle \psi^E_{\{n,l,m\}}(r_{12}, r_{34}, r_{1234}) |\, \chi^E_{\{n',l',m'\}}(r_{14}, r_{32}, r_{1432}) \rangle \langle \chi^E_{\{n',l',m'\}}(r_{14}, r_{32}, r_{1432}) \,| \, .$$

Now we define a transformation matrix $D^E_{\{\{n,l,m\},\{n',l',m'\}\}}$ as

$$D^E_{\{\{n,l,m\},\{n',l',m'\}\}} =$$
$$\int dr_{14} \int dr_{23} \int dr_{1234} \langle \psi^E_{\{n,l,m\}}(r_{12}, r_{34}, r_{1234}) \mid \chi^E_{\{n',l',m'\}}(r_{14}, r_{32}, r_{1432}) \rangle,$$

for which the following analytical expression was obtained in Ref.:[25]

$$\mathcal{D}^E_{\{\{n,\ell,m\},\{n',\ell',m'\}\}}\left(\{\mathbf{r}\}\,;\,\{\mathbf{r}'\}\right) = \tag{2·19}$$
$$\left(\frac{\pi}{4}\right)^{\frac{1}{2}N(N-1)} \left\{ \prod_{i=1}^{N} (-1)^{n_i} \left[\frac{\Gamma\left(n_i+1\right)\Gamma\left(n_i+\ell_i+\frac{3}{2}\right)}{2\ell_i+1} \right]^{1/2} \right\}$$

$$\left\{\prod_{j=1}^{N}(-1)^{n'_j}\left[\frac{\Gamma\left(n'_j+1\right)\Gamma\left(n'_j+\ell'_j+\frac{3}{2}\right)}{2\ell'_j+1}\right]^{1/2}\right\}\sum_{n_{ij},\ell_{ij},m_{ij}}$$
$$\left[\left\{\prod_{i=1}^{N}\delta\left(\sum_{j=1}^{N}\left(2n_{ij}+\ell_{ij}\right),2n'_i+\ell'_i\right)\left(\begin{array}{ccc|c}\ell_{i1}&\cdots&\ell_{iN}&\ell'_i\\ m_{i1}&\cdots&m_{iN}&m'_i\end{array}\right)\right\}\right.$$
$$\left\{\prod_{j=1}^{N}\delta\left(\sum_{i=1}^{N}\left(2n_{ij}+\ell_{ij}\right),2n_j+\ell_j\right)\left(\begin{array}{ccc|c}\ell_{1j}&\cdots&\ell_{Nj}&\ell_j\\ m_{1j}&\cdots&m_{Nj}&m_j\end{array}\right)\right\}$$
$$\left.\left\{\prod_{i=1}^{N}\prod_{j=1}^{N}\left(\alpha_{ij}\right)^{2n_{ij}+\ell_{ij}}\frac{2\ell_{ij}+1}{\Gamma\left(n_{ij}+1\right)\Gamma\left(n_{ij}+\ell_{ij}+\frac{3}{2}\right)}\right\}\right]. \tag{2·20}$$

We denote the elements of this transition D-matrix by g_n, which give the probability of the transition from a particular meson channel to a particular quark channel, and vice versa. These g_n precisely correspond to the overlap wave functions $\sqrt{a}/\mu_c\langle|\vec{r_f}|\mid n_c,l_c,m_c\rangle$ in Eq. (2·15). Replacing these overlap functions by $\mu_c g_n/(\sqrt{a})$ turns Eq. (2·15) into

$$\begin{aligned}\langle\vec{P}_f\mid V_{MM}\mid\vec{P}'_f\rangle&=\frac{a^4}{(2\pi)^3}\sum_{n_c,l_c,m_c}\int d\Omega_{r_f}\int d\Omega_{rf'}e^{-i\vec{P}_f\cdot a\hat{r}_f}\left(\frac{\lambda}{\mu_c a}\right)^2\frac{\mu_c^2 g_n^2}{a}\times\\&\quad\times\frac{Y^{l_f}_{m_f}(\hat{r_f})Y^{l_f}_{m_f}(\hat{r_f}')}{E(\vec{P}_f)-E_{nl}}e^{i\vec{P}'_f\cdot a\hat{r}'_f}\\&=\frac{\lambda^2 a}{(2\pi)^3}\sum_{n_c,l_c,m_c}\int d\Omega_{r_f}\int d\Omega_{r'_f}e^{-i\vec{P}_f\cdot a\hat{r}_f}Y^{l_f}_{m_f}(\hat{r_f})Y^{l_f}_{m_f}(\hat{r_f}')\times\\&\quad\times\frac{g_n^2}{E(\vec{P}_f)-E_{nl}}e^{i\vec{P}'_f\cdot a\hat{r}'_f}.\end{aligned} \tag{2·21}$$

Using the standard relations for spherical harmonics

$$\int d\Omega_{r_f}e^{-i\vec{P}_f.\hat{r}_f a}Y^{l_f}_{m_f}(\hat{r}_f)=(-i)^l_f 4\pi j_l(P_f a)Y^{l_f}_{m_f}(\hat{P}_f) \tag{2·22}$$

in Eq. (2·21), we get

$$\begin{aligned}&\langle\vec{P}_f\mid V_{MM}\mid\vec{P}'_f\rangle\;=\\&\quad=\frac{\lambda^2 a}{(2\pi)^3}\sum_{n_c,l_c,m_c}(-i)^{l_f}4\pi j_l(P_f a)Y^{l_f}_{m_f}(\hat{P}_f)(i)^{l_f}4\pi j_l(P'_f a)Y^{*l_f}_{m_f}(\hat{P}'_f)\frac{g_n^2}{E(\vec{P}_f)-E_{nl}}\\&\quad=\frac{\lambda^2 a}{(2\pi)^3}\sum_{n_c,l_c,m_c}(-i^2)^{l_f}(4\pi)^2 j_l(P_f a)j_l(P'_f a)Y^{l_f}_{m_f}(\hat{P}_f)Y^{*l_f}_{m_f}(\hat{p}'_f)\frac{g_n^2}{E(\vec{P}_f)-E_{nl}}\end{aligned}$$

$$= \frac{\lambda^2 a}{(2\pi)^3} \sum_{n_c,l_c} (-i^2)^{l_f} (4\pi)^2 j_l(P_f a) j_l(P'_f a) \frac{2l_f+1}{4\pi} \mathbb{P}_{l_f}(\hat{P}_f \cdot \hat{P}'_f) \frac{g_n^2}{E(\vec{P}_f) - E_{nl}}$$

$$= \frac{\lambda^2 a}{2\pi^2} \sum_{l_c=0}^{\infty} (2l_f+1) \mathbb{P}_{l_f}(\hat{P}_f \cdot \hat{P}'_f) j_l(P_f a) j_l(P'_f a) \sum_{n_c=0}^{\infty} \frac{g_n^2}{E(\vec{P}_f) - E_{nl}}, \tag{2·23}$$

where $\mathbb{P}_l(x)$ is the Legendre polynomial.

Using this potential, a simple closed-form expression for the S-matrix can be obtained, if only one confined and one free channel are considered (see Appendices A.1–A.5 of Ref.[51] for a detailed derivation), viz.

$$S_{l_f}(E) = 1 - 2i \frac{2a\lambda^2 \sum\limits_{n=0}^{\infty} \frac{g_n^2}{E(\vec{P}_f) - E_{nl}} \mu_f P_f j_{l_f}(P_f a) h^1_{l_f}(P_f a)}{1 + 2ia\lambda^2 \sum\limits_{n=0}^{\infty} \frac{g_n^2}{E(\vec{P}_f) - E_{nl}} \mu_f P_f j_{l_f}(P_f a) h^1_{l_f}(P_f a)}. \tag{2·24}$$

An exact solution for the S-matrix can be derived in the most general multichannel case as well, resulting in a matrix expression with a similar structure.[31]

The full scattering amplitude can be depicted diagrammatically as shown in Fig. 4, where the shaded boxes represent the effective meson-meson potential depicted in Fig. 1.

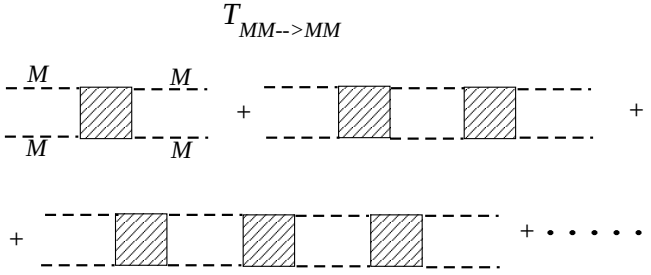

Fig. 4. The full scattering amplitude for two mesons, with the shaded boxes given by Fig. 1.

In order to find resonances in non-exotic meson-meson systems, we search for zeros in the denominator of the S-matrix (Eq. (2·24)), which correspond to poles in the complex-energy plane. Then we vary the parameters λ and a to fit the experimental data for a particular case. We also study the pole movements in the complex plane, as we change the parameter λ, in order to get more physical insight into the model, and to evaluate the role of meson loops coupled to quark channels in the generation of resonances.

§3. Perturbative formalism

The main purpose of this paper is to show that predictions of resonances poles based on perturbative calculations in standard quark models can be very misleading. In order to demonstrate this in a quantitative way, we now construct a perturbative scheme for the formalism described in the previous section.

As explained above, the λ in our formalism is the coupling of the meson-meson $\leftrightarrow$ $q\bar{q}$ vertex. The term corresponding to λ^2 thus represents the lowest-order meson-meson interaction (meson-meson $\rightarrow$ $q\bar{q}$ $\rightarrow$ meson-meson). The position of a pole in a particular case of meson-meson scattering, above threshold, can be expanded perturbatively in terms of λ^2 as

$$E_m^{\rm pole} = E_m + \lambda^2 E_m^{\rm LO} + \lambda^4 E_m^{\rm NLO} + \lambda^6 E_m^{\rm NNLO} + \ldots . \tag{3·1}$$

The first term of this series corresponds to the confinement pole, which is what we should get from the model if the coupling of the quark pair to the meson channels vanished. The second term is the leading-order term in λ^2. The denominator of the S-matrix (Eq. (2·24)), written up to leading order in λ^2 around the mth confinement pole, becomes

$$1 + 2ia\lambda^2 \frac{g_m^2}{E_m + \lambda^2 E_m^{\rm LO} - E_m} \mu k j_l(ka) h_l^1(ka) = 0, \tag{3·2}$$

which then yields

$$E_m^{\rm LO} = -2ia g_m^2 \mu k j_l(ka) h_l^1(ka). \tag{3·3}$$

So the pole position (Eq. (3·1)), in lowest-order approximation, is

$$E_m^{\rm pole} \approx E_m - 2ia g_m^2 \mu k j_l(ka) h_l^1(ka). \tag{3·4}$$

We now expand the denominator of Eq. (2·24) to higher order in λ^2. In order to do so, we define

$$f(\lambda^2) = 2ia\mu k j_l(ka) h_l^1(ka), \tag{3·5}$$

such that Eq. (2·24) becomes

$$S_l(E) = 1 - \frac{2\lambda^2 f(\lambda^2) \sum\limits_{n=0}^{\infty} \frac{g_n^2}{E - E_n}}{1 + \lambda^2 f(\lambda^2) \sum\limits_{n=0}^{\infty} \frac{g_n^2}{E - E_n}}. \tag{3·6}$$

Now we expand the function f around the energy $E = E_m$, i.e., around $\lambda = 0$, as

$$\begin{aligned} f(E_m) &= f(E_m) + \lambda^2 \frac{\partial f}{\partial \lambda^2}\Big|_{\lambda=0} + \frac{1}{2}\lambda^4 \frac{\partial^2 f}{\partial (\lambda^2)^2}\Big|_{\lambda=0} + \frac{1}{6}\lambda^6 \frac{\partial^3 f}{\partial (\lambda^2)^3}\Big|_{\lambda=0} \\ &\quad + \ldots \\ &= f(E_m) + \lambda^2 \frac{\partial f}{\partial E}\frac{\partial E}{\partial \lambda^2}\Big|_{\lambda=0} + \frac{1}{2}\lambda^4 \left[\frac{\partial^2 f}{\partial E^2} \left(\frac{\partial E}{\partial \lambda^2} \right)^2 \right. \\ &\quad \left. + \frac{\partial f}{\partial E}\frac{\partial^2 E}{\partial \lambda^2} \right]_{\lambda=0} + \frac{1}{6}\lambda^6 \left[\frac{\partial^3 f}{\partial E^3} \left(\frac{\partial E}{\partial \lambda^2} \right)^3 + 3\frac{\partial^2 f}{\partial E^2}\frac{\partial E}{\partial \lambda^2}\frac{\partial^2 E}{\partial (\lambda^2)^2} \right. \qquad (3·7) \\ &\quad \left. + \frac{\partial f}{\partial E}\frac{\partial^3 E}{\partial (\lambda^2)^3} \right]_{\lambda=0} + \ldots . \qquad (3·8) \end{aligned}$$

From Eq. (3·1), we have $E_m^{\rm pole}|_{\lambda=0} = E_m$, and

$$\frac{\partial E_m^{\rm pole}}{\partial \lambda^2}\Big|_{\lambda=0} = E_m^{\rm LO},\ \frac{\partial^2 E_m^{\rm pole}}{\partial (\lambda^2)^2}\Big|_{\lambda=0} = 2E_m^{\rm NLO},\ \frac{\partial^3 E_m^{\rm pole}}{\partial (\lambda^2)^3}\Big|_{\lambda=0} = 6E_m^{\rm NNLO},\ \ldots.$$

Using these relations in Eq. (3·8), we get

$$\begin{aligned} f(E_m) = f(E_m) &+ \lambda^2 E_m^{\rm LO}\frac{\partial f}{\partial E}\Big|_{E=E_m} \\ &+ \frac{1}{2}\lambda^4\left[\left(E_m^{\rm LO}\right)^2\frac{\partial^2 f}{\partial E^2}\Big|_{E=E_m} + 2E_m^{\rm NLO}\frac{\partial f}{\partial E}\Big|_{E=E_m}\right] \\ &+ \frac{1}{6}\lambda^6\left[\left(E_m^{\rm LO}\right)^2\frac{\partial^3 f}{\partial E^3}\Big|_{E=E_m} + 6E_m^{\rm NLO}E_m^{\rm LO}\frac{\partial^2 f}{\partial E^2}\Big|_{E=E_m}\right] \\ &+ 6E_m^{\rm NNLO}\frac{\partial f}{\partial E}\Big|_{E=E_m} + \ldots. \end{aligned} \tag{3·9}$$

It remains to consider the remaining part of the denominator, namely

$$\lambda^2\sum_{n=0}^{\infty}\frac{g_n^2}{E-E_n} = \lambda^2\sum_{n\neq m}^{\infty}\frac{g_n^2}{E-E_n} + \lambda^2\frac{g_m^2}{E-E_m}, \tag{3·10}$$

which we expand in a series in λ^2, around $\lambda = 0$ (so at $E = E_m$), in a similar way as the function f, to obtain

$$\begin{aligned} \lambda^2\sum_{n=0}^{\infty}\frac{g_n^2}{E-E_n} &= \lambda^2\sum_{n\neq m}\frac{g_n^2}{E_m-E_n} - \lambda^4 E_m^{\rm LO}\sum_{n\neq m}\frac{g_n^2}{(E_m-E_n)^2} \\ &+\lambda^6\left\{(E_m^{\rm LO})^2\sum_{n\neq m}\frac{g_n^2}{(E_m-E_n)^3} - E_m^{\rm NLO}\sum_{n\neq m}\frac{g_n^2}{(E_m-E_n)^2}\right\} \\ &+g_m^2\left[\frac{1}{E_m^{\rm LO}} - \lambda^2\frac{E_m^{\rm NLO}}{(E_m^{\rm LO})^2} + \lambda^4\left\{\frac{(E_m^{\rm NLO})^2}{(E_m^{\rm LO})^3} - \frac{E_m^{\rm NNLO}}{(E_m^{\rm LO})^2}\right\}\right] \\ &+g_m^2\left[-\lambda^6\left\{\frac{(E_m^{\rm NLO})^3}{(E_m^{\rm LO})^4} - 2\frac{E_m^{\rm NLO}*E_m^{\rm NNLO}}{(E_m^{\rm LO})^3} + \frac{E_m^{\rm N^3LO}}{(E_m^{\rm LO})^2}\right\}\right] + \ldots. \end{aligned} \tag{3·11}$$

Upon multiplying Eqs. (3·9) and (3·11), we get an expansion in λ^2 for the pole position, viz.

$$\begin{aligned} 0 &= 1 + g_m^2 E_m^{\rm LO} f(E_m) \\ &+ \lambda^2\left\{\left(\sum_{n\neq m}\frac{g_n^2\left(E_m^{\rm LO}\right)^2}{E_m-E_n} - g_m^2 E_m^{\rm NLO}\right)\frac{f(E_m)}{\left(E_m^{\rm LO}\right)^2} + g_m^2\frac{\partial f}{\partial E}\Big|_{E=E_m}\right\} \\ &+ \lambda^4\left\{\left(-\sum_{n\neq m}\frac{g_n^2\left(E_m^{\rm LO}\right)^4}{(E_m-E_n)^2} + g_m^2\left\{\left(E_m^{\rm NLO}\right)^2 - E_m^{\rm LO}E_m^{\rm NNLO}\right\}\right)\frac{f(E_m)}{(E_m^{\rm LO})^3}\right. \end{aligned}$$

$$
\begin{aligned}
&+\left(\sum_{n\neq m}\frac{g_n^2 E_m^{\rm LO}}{E_m-E_n}\right)\frac{\partial f}{\partial E}\Big|_{E=E_m}+\frac{1}{2}g_m^2 E_m^{\rm LO}\frac{\partial^2 f}{\partial E^2}\Big|_{E=E_m}\Bigg\}\\
&+\lambda^6\Bigg\{\Bigg(\sum_{n\neq m}\frac{g_n^2\left(E_m^{\rm LO}\right)^6}{(E_m-E_n)^3}-\sum_{n\neq m}\frac{g_n^2\left(E_m^{\rm LO}\right)^4 E_m^{\rm NLO}}{(E_m-E_n)^2}\\
&-g_m^2\left\{\left(E_m^{\rm NLO}\right)^3-2E_m^{\rm NLO}E_m^{\rm NNLO}E_m^{\rm LO}+E_m^{\rm N^3LO}\left(E_m^{\rm LO}\right)^2\right\}\Bigg)\frac{f(E_m)}{\left(E_m^{\rm LO}\right)^4}\\
&+\left(-\sum_{n\neq m}\frac{g_n^2\left(E_m^{\rm LO}\right)^2}{(E_m-E_n)^2}+\sum_{n\neq m}\frac{g_n^2 E_m^{\rm NLO}}{E_m-E_n}\right)\frac{\partial f}{\partial E}\Big|_{E=E_m}+\\
&+\frac{1}{2}\left(\sum_{n\neq m}\frac{g_n^2\left(E_m^{\rm LO}\right)^2}{E_m-E_n}+g_m^2E_m^{\rm NLO}\right)\frac{\partial^2 f}{\partial E^2}\Big|_{E=E_m}\\
&+\frac{1}{6}g_m^2\left(E_m^{\rm LO}\right)^2\frac{\partial^3 f}{\partial E^3}\Big|_{E=E_m}\Bigg\}.
\end{aligned}
$$

Solving this equation order by order in λ^2, we obtain the expressions for e.g. the pole position to lowest order, next-to-lowest order, and next-to-next-to-lowest order as

$$E_m^{\rm LO}=-g_m^2 f(E_m), \tag{3·12}$$

$$E_m^{\rm NLO}=g_m^4 f(E_m)\frac{\partial f}{\partial E}\Big|_{E=E_m}+g_m^2 f^2(E_m)\sum_{n\neq m}\frac{g_n^2}{E_m-E_n}, \tag{3·13}$$

$$
\begin{aligned}
E_m^{\rm NNLO}&=g_m^4 f^3(E_m)\sum_{n\neq m}\frac{g_n^2}{(E_m-E_n)^2}-g_m^2 f^3(E_m)\times\\
&\left(\sum_{n\neq m}\frac{g_n^2}{E_m-E_n}\right)^2-3g_m^4 f^2(E_m)\frac{\partial f}{\partial E}\Big|_{E=E_m}\left(\sum_{n\neq m}\frac{g_n^2}{E_m-E_n}\right)\\
&-\frac{1}{2}g_m^6 f^2(E_m)\frac{\partial^2 f}{\partial E^2}\Big|_{E=E_m}-g_m^6 f(E_m)\left(\frac{\partial f}{\partial E}\Big|_{E=E_m}\right)^2.
\end{aligned}
\tag{3·14}
$$

Similarly, one can obtain the expressions for even higher-order contributions.

§4. Results and discussion

To test the validity of the perturbative calculus, we now choose a few concrete examples of meson-meson systems, namely $K\pi$ in P wave, $D\bar{D}$ in P wave, and DK in S wave. First we compute the scattering poles in these systems by using the exact formalism, explained in Sect. 2. In particular, we study the S-matrix (Eq. (2·24)) pole positions in the complex-energy plane, as a function of the coupling λ. The resulting pole trajectories behave as expected from general considerations:

- The unperturbed, or bare, quark-antiquark spectrum is given by Eq. (2·11). For small coupling to the scattering sector, we must find resonance poles close to the levels of this spectrum.
- For larger coupling, the resonances are expected to acquire larger widths, so the pole positions must get larger (negative) imaginary parts. However, associated with larger widths are, in general, larger mass shifts. As a consequence, also the real parts of the pole positions will deviate substantially from the levels of the bare $q\bar{q}$ spectrum.
- Sometimes, a further increased coupling may lead to a sufficiently large mass shift so as to push the pole below the scattering threshold. For such a situation, we expect a bound state. Since a bound state has zero width, the pole should eventually end up on the real-energy axis.

Next, we study the same cases, but now using the perturbative formalism derived in Sect. 3, up to fourth order in λ^2. This way we can compare exact and perturbative results for the real and imaginary mass shifts due to meson loops. The latter quantities are related to predictions for the central resonance masses and resonance widths. We will find that, for moderate to large couplings, the perturbative results strongly deviate from and do not converge towards the exact ones. In particular, the expected behavior of poles below the scattering threshold, namely to move towards or along the real-energy axis, cannot be reproduced at all by the studied perturbative expansions.

In all cases we will employ the quark masses $m_n \equiv m_u = m_d = 0.406$ GeV, $m_s = 0.508$ GeV, $m_c = 1.562$ GeV, as well as the universal oscillator frequency $\omega = 0.19$ GeV, all determined in the model of Ref.[17] The values of the parameters a and λ are given separately for each case in the following discussion.

The parameter a in Eq. (2·14) describes the average distance at which quark-pair creation or annihilation takes place, leading to the two-meson decay of a meson. For the case of $K\pi$, which is a nonstrange-strange flavor combination, we choose here $a = 2.534$ GeV^{-1}. This is smaller than the value $a = 3.2$ GeV^{-1}, which would be used in a multichannel fit to several mesons. The reason for this discrepancy is that one meson-meson channel, namely $K\pi$, has to mimic the effect of a multichannel treatment. In order to nonetheless obtain the $K^*(892)$ pole at a reasonable position, we have to adjust the parameter a. In the $D\bar{D}$ and DK cases, we use here values close to the ones used in a multichannel calculation,[17] namely $a = 1.72$ GeV^{-1} and $a = 2.5$ GeV^{-1}, respectively. The price we pay is that, in the $D\bar{D}$ case, the $\psi(2S)$ pole does not come out at 3.686 GeV, but about 40–50 MeV higher.

For the parameter λ, which is the universal overall three-meson coupling constant, we could have used, after scaling, the same value in all three cases. However, scaling was not carried out[52] in the DK case, which makes that the pole now greatly overshoots the $D_{s0}(2317)$ position for $\lambda = 1$. With the correct scaling, it would end up roughly 20 MeV too high.

One might argue that only one value of the coupling λ describes the physical situation, so that other values are not relevant. However, as analyticity has proven in the past to be a powerful tool for constructing scattering amplitudes, the trajectories of their poles are also a strong indication for the correctness of their dependence on

other parameters. In the following, we will show that perturbative expansions, even to higher orders, only have a very limited range of validity, and do not cover the realistic case of large couplings[34),36),53)] in strong interactions.

4.1. *P-wave $K\pi$ scattering*

The $K^*(892)$ resonance is well described by a Breit-Wigner resonance in P-wave $K\pi$ scattering, with central mass and resonance width of about 892 MeV and 50 MeV, respectively. Hence, we expect a pole in the S matrix of Eq. (2·24) for an S-wave nonstrange-strange quark-antiquark system, coupled to a P-wave kaon-pion meson-meson system. For the couplings g_n we find[25)] in this case

$$g_n = 2^{-n} \left(\frac{2n+3}{3} \right)^{1/2} . \tag{4·1}$$

Scattering poles are obtained by studying the zeros of the denominator in the expression of Eq. (2·24). In Fig. 5(a), we depict the S-matrix pole positions for a range of λ values varying from 0 to just over 2.

In the limit of vanishing coupling, one expects to find the poles at the bare masses of the quark-antiquark system, as given by Eq. (2·11). We obtain from Eq. (2·11) the value $E_{00} = 1.199$ GeV for the ground-state bare mass, which indeed corresponds to the limit of vanishing λ along the dashed curve in Fig. 5(a). For larger couplings, we observe that the imaginary part of the pole position vanishes at the $K\pi$ threshold. This was to be expected, since a large coupling results in a bound state below the $K\pi$ threshold, which of course has a zero width. The shape of the pole trajectory near the $K\pi$ threshold is in accordance with theory for poles in P-wave scattering and also in higher partial waves.[54),55)] For S-wave scattering the pole behavior is different, as we will see in Sect. 4.3, but again in agreement with theory.[54),55)]

The value $\lambda = 1$ corresponds to the physical pole, as it roughly reproduces the characteristics of the K^* (892) resonance. In the present simplified model, the pole comes out at $(0.972 - i0.026)$ GeV, as shown in Fig. 5(a).

The coefficients of the perturbative expansion (Eq. (3·1)) are collected in Table I, for the case of P-wave $K\pi$ scattering. In Figs. 5(b–f) we depict the perturbative pole

coefficient	value (GeV)
E_0	(1.199, 0.)
$E_0^{\mathrm{N^0LO}}$	(-0.249080686,-0.0878366188)
$E_0^{\mathrm{N^1LO}}$	(-0.0435913117,0.0471697828)
$E_0^{\mathrm{N^2LO}}$	(0.0631440181,0.0973648258)
$E_0^{\mathrm{N^3LO}}$	(0.0869057944,-0.0785515047)
$E_0^{\mathrm{N^4LO}}$	(-0.067527691,-0.0632886834)

Table I. Coefficients of the perturbative expansion given in Eq. (3·1), concerning the pole positions of the ground-state pole in P-wave $K\pi$ scattering.

trajectories for the bare nonstrange-strange $q\bar{q}$ state at 1.199 GeV. Shown are the

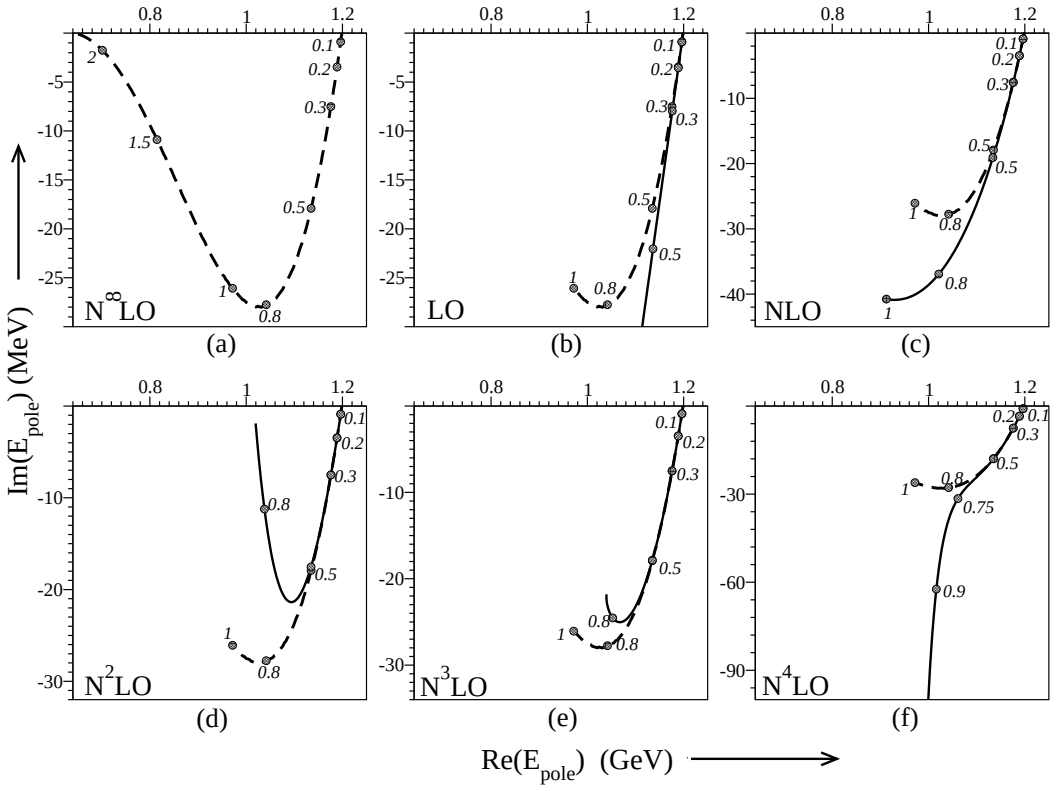

Fig. 5. The P-wave $K\pi$ resonance pole positions in the complex-energy plane, corresponding to the second Riemann sheet, under variation of the coupling λ. The dashed curves in all the plots for $\mathrm{N}^n\mathrm{LO}$ ($n = 0, \ldots, 4$) are the same as the ones shown for $\mathrm{N}^\infty\mathrm{LO}$ (labeled (a)). The solid curves are the results obtained from the perturbative approximations, viz. (b) leading ($\mathrm{N}^0\mathrm{LO}$, Born) term, (c) next-to-leading ($\mathrm{N}^1\mathrm{LO}$), (d) next-to-next-to-leading ($\mathrm{N}^2\mathrm{LO}$), (e) (next-to)^3-leading ($\mathrm{N}^3\mathrm{LO}$) and (f) (next-to)^4-leading ($\mathrm{N}^4\mathrm{LO}$) orders, respectively.

curves for the lowest-order (Born) term ($E_0^{\mathrm{N}^0\mathrm{LO}}$) and for the next few higher-order terms ($E_0^{\mathrm{N}^1\mathrm{LO}}$, ...), respectively, up to fourth order in λ^2. We find that the Born term gives satisfactory pole positions for overall couplings up to $\lambda \approx 0.3$. At each higher order, the perturbative pole positions, i.e., the central masses and the widths of the $K^*(892)$ resonance, are better and better determined, up to $\lambda \approx 0.75$ for the fourth-order approximation. However, thereabove things go terribly wrong, and all approximations completely fail to reproduce the physical pole at $\lambda = 1$.

So we are forced to conclude that perturbation theory is unreliable to describe the $K^*(892)$ resonance. Moreover, we should add that these higher-order perturbative calculations are much more tedious than just finding the exact solution for the coupled quark-antiquark and meson-meson system.

4.2. *P-wave $D\bar{D}$ scattering*

Let us next consider the $D\bar{D}$ system, which has been studied already a long time ago,[16] using the model described in Sect. 2. In Ref.[16] it was shown that the P-wave $D\bar{D}$ channel, together with higher open-charm channels, can transform the bare vector charmonium spectrum into the physical one. In particular, the pole stemming from the first radial excitation comes out very close to the $\psi(2S)(3686)$ state, which turns out to contain a significant $D\bar{D}$ component, besides $c\bar{c}$ of course.

The couplings g_n in this case are again given by the vector $\leftrightarrow$ pseudoscalar-pseudoscalar vertex, for which we use the same expression as in Eq. (4·1). The parameter a is now taken at 0.34 fm. Using these inputs, the S-matrix (Eq. (2·24)) is calculated, and we search for poles on the second Riemann sheet. We present the results of our calculation in Fig. 6(a), which depicts the complex-energy plane around the mass of the $\psi(2S)(3686)$. The dashed line in Fig. 6(a) corresponds to

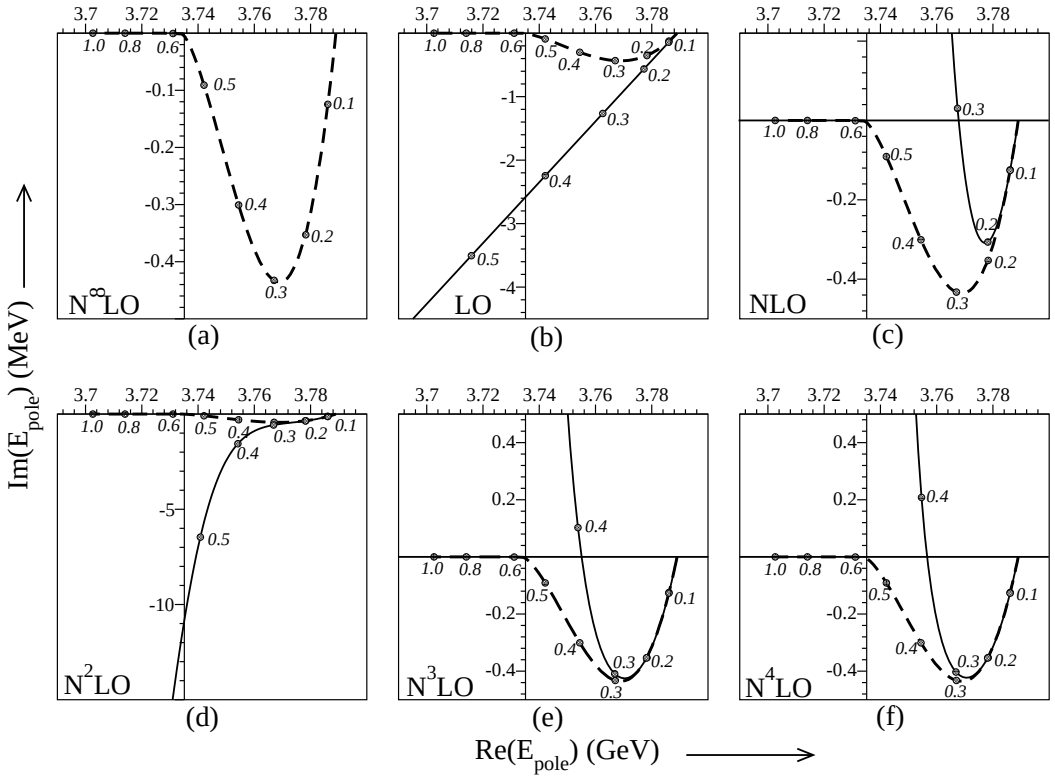

Fig. 6. P-wave $D\bar{D}$ pole positions in the complex-energy plane (corresponding to the first and second Riemann sheets), under variation of the coupling λ. The dashed curves in all the plots for $\mathrm{N}^n\mathrm{LO}$ ($n = 0, \ldots, 4$) are the same as the one for $\mathrm{N}^\infty\mathrm{LO}$ (labeled (a)). The solid curves represent the perturbative results: (b) leading ($\mathrm{N}^0\mathrm{LO}$, Born) term, (c) next-to-leading ($\mathrm{N}^1\mathrm{LO}$), (d) next-to-next-to-leading ($\mathrm{N}^2\mathrm{LO}$), (e) (next-to)^3 ($\mathrm{N}^3\mathrm{LO}$), and (f) (next-to)^4-leading ($\mathrm{N}^4\mathrm{LO}$) orders, respectively.

the movement of the pole in the complex plane between the $D\bar{D}$ threshold and the

first radial excitation of the J/ψ, as λ is varied between the limiting values 0 and 1. As expected, when the coupling is very small, we find a pole close to the first radial excitation of the confined $c\bar{c}$ spectrum of the model, i.e., near $E_1 = \omega(2+3/2)+2m_c = 3.789$ GeV (Eq. (2·11)). As λ is increased to 0.1, the real part of the pole becomes $\Re\mathrm{e}(E) \simeq 3.77$ GeV Finally, for $\lambda \simeq 1$, the pole is found below the $D\bar{D}$ threshold, very close to 3.7 GeV, which should corresponds to the physical $\psi(2S)(3686)$.

Next we show the pole positions obtained in the perturbative expansion, viz. from Eqs. (3·12–3·14)) and similar expressions up to fourth order in λ^2. The coefficients of Eq. (3·1) are collected in Table II.

coefficient	value (GeV)
E_0	(3.789, 0.)
$E_0^{\mathrm{N^0LO}}$	(-0.291265968,-0.0139626856)
$E_0^{\mathrm{N^1LO}}$	(0.587237403,0.157827196)
$E_0^{\mathrm{N^2LO}}$	(-0.763203829,-0.81585325)
$E_0^{\mathrm{N^3LO}}$	(-0.589315239,2.48140259)
$E_0^{\mathrm{N^4LO}}$	(7.66667227,0.981322456)

Table II. Coefficients of the perturbative expansion (Eq. (3·1)) for the first radially excited pole in P-wave DD scattering.

Figure 6(b) shows that the pole position found in the leading-order approximation agrees with the full calculation only for very small values of λ, but as the coupling increases, the approximate pole starts to deviate strongly from the exact one shown in Fig. 6(a). For example, at $\lambda = 0.5$, the first-order pole comes out below threshold but with a large imaginary part, which is obviously unphysical. For the higher-order approximations, the results are even worse, with the pole moving into the upper half plane, or extremely deep down in the lower half for the $\mathrm{N^2LO}$ case. It becomes evident that no perturbative approximation will produce anything even resembling a bound-state pole for $\lambda \sim 1$.

4.3. *DK S-wave scattering*

Finally, we study the case of S-wave DK scattering taking

$$g_n = 2^{-n}\,(n+1)^{1/2}\,. \tag{4·2}$$

Now, as one can see in Fig. 7(a), the shape of the pole trajectory near the DK threshold is very different from the two P-wave cases. For increasing λ, the pole approaches the real-energy axis below threshold, moves along the axis towards threshold as a virtual bound state, and then becomes a bound state, moving finally to lower and lower energies. There is a one-to-one relation of this complex-energy pole trajectory to the equivalent one in the complex-momentum plane. Thus, a virtual bound state moving towards threshold corresponds to a momentum pole moving upwards along the negative imaginary axis, passing through the origin when the virtual bound state becomes a true bound state, at threshold. In the present case, the pole is still on

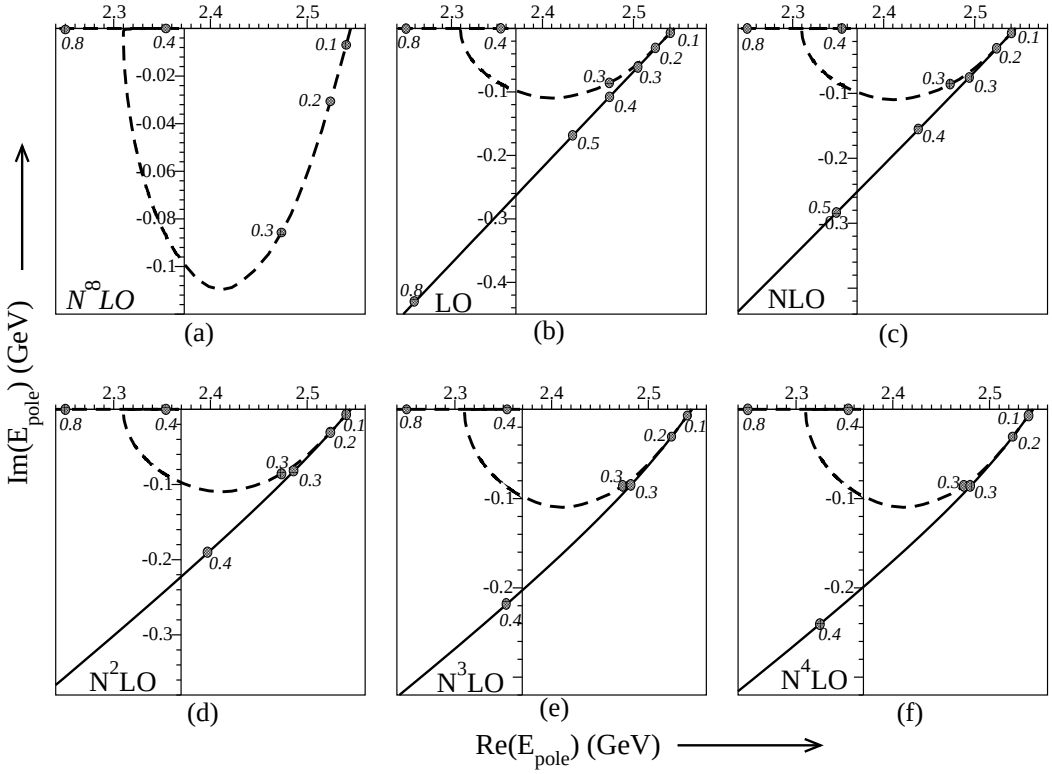

Fig. 7. S-wave DK pole positions in the complex-energy plane (corresponding to the first and second Riemann sheets), under variation of the coupling λ. The dashed curves in all the plots for $\mathrm{N}^n\mathrm{LO}$ ($n = 0, \ldots, 4$) are the same as the one for $\mathrm{N}^\infty\mathrm{LO}$ (labeled (a)). The solid curves represent the perturbative results: (b) leading ($\mathrm{N}^0\mathrm{LO}$, Born) term, (c) next-to-leading ($\mathrm{N}^1\mathrm{LO}$), (d) next-to-next-to-leading ($\mathrm{N}^2\mathrm{LO}$), (e) (next-to)^3 ($\mathrm{N}^3\mathrm{LO}$), and (f) (next-to)^4-leading ($\mathrm{N}^4\mathrm{LO}$) orders, respectively.

the negative imaginary axis for $\lambda = 0.4$, but already on the positive one for $\lambda = 0.5$. This phenomenon, which happens exclusively for S-wave scattering, as can be seen from the effective-range expansion, is well described in Refs.[54),55)] For $\lambda \approx 0.6$, the bound-state pole reproduces the $D_{s0}(2317)$ mass.

The coefficients of Eq. (3·1) for the case of S-wave DK scattering are collected in Table III. One sees at a glance that these coefficients do not promise any kind of convergence. Indeed, upon inspecting Figs. 7(b–f), one notices that only for small values of λ the perturbative pole positions agree with the exact ones. However, for $\lambda \geq 0.3$, the discrepancies grow rapidly, and no significant improvement is observed for higher orders of perturbation theory.

§5. Summary and conclusions

We have studied the discrepancies between perturbative estimates for resonance pole positions and the exact ones, in the context of a simple soluble model for

coefficient	value (GeV)
E_0	(2.545,0.)
$E_0^{\mathrm{N^0LO}}$	(-0.445872986,-0.67333385)
$E_0^{\mathrm{N^1LO}}$	(-1.36316635,-1.84200144)
$E_0^{\mathrm{N^2LO}}$	(-9.95402765,-8.57593239)
$E_0^{\mathrm{N^3LO}}$	(-68.4326606,-43.6873369)
$E_0^{\mathrm{N^4LO}}$	(-299.284654,-138.032657)

Table III. Coefficients of the perturbative expansion (Eq. (3·1)) for the ground-state pole in S-wave DK scattering.

hadronic decay of a meson. In none of the considered cases satisfactory results were obtained with the perturbative method, and not even any significant improvement was found for increasing orders of perturbation theory. In particular, for bound states below the lowest strong-decay threshold, no perturbative approximation produced anything like a pole close to the real-energy axis. But also in the case of a normal and not even very broad resonance, namely the $K^*(892)$, the perturbative approach failed completely.

These results should be a warning for quark-model builders, because of two reasons. First of all, the found large real mass shifts are, as a consequence of analyticity, inseparably connected to the generation of the physical hadronic widths, as demonstrated here for the $K^*(892)$, but shown already many years ago for a variety of mesons,[17] and confirmed in several more recent papers referred to above. Therefore, any spectroscopic conclusions based on single-channel, "quenched" quark models should be taken with a great deal of caution. The second reason is that even those quark models which pay some attention to strong decay, usually do this by employing perturbative methods. The results presented here make it clear that a completely non-perturbative treatment of hadronic resonances and bound states is required for a realistic description.

Acknowledgments

This work was supported in part by the *Fundação para a Ciência e a Tecnologia* of the *Ministério da Ciência, Tecnologia e Ensino Superior* of Portugal, under contract CERN/FP/109307/2009.

References

1) W. Dunwoodie [BaBar Collaboration], Nucl. Phys. A **827** (2009), 291C.
2) S. Tosi [BaBar Collaboration], *Prepared for 18th International Conference on Particles and Nuclei (PANIC 08), Eilat, Israel, 9–14 Nov 2008.*
3) K. F. Chen [Belle Collaboration], arXiv:0810.3829.
4) S. K. Choi [Belle Collaboration], AIP Conf. Proc. **1182** (2009), 455.
5) A. Zupanc [Belle Collaboration], arXiv:0910.3404.
6) X. Ji [BES Collaboration], published in *La Thuile 2002, Results and perspectives in particle physics*, 569–577.

7) J. Chen [BES Collaboration], Nucl. Phys. Proc. Supp. **186** (2009), 371.
8) A. Tomaradze [CLEO Collaboration], AIP Conf. Proc. **1257** (2010), 197, arXiv:1001.2252.
9) K. K. Seth, arXiv:0912.2704.
10) R. D. Matheus, F. S. Navarra, M. Nielsen and C. M. Zanetti, Phys. Rev. D **80** (2009), 056002, arXiv:0907.2683.
11) M. Nielsen, F. S. Navarra and S. H. Lee, arXiv:0911.1958.
12) G. J. Ding and M. L. Yan, Phys. Lett. B **657** (2007), 49, hep-ph/0701047.
13) T. Hyodo, D. Jido and A. Hosaka, Phys. Rev. C **78** (2008), 025203, arXiv:0803.2550.
14) F. Giacosa, Phys. Rev. D **80** (2009), 074028, arXiv:0903.4481.
15) E. van Beveren and G. Rupp, Annals. Phys. **323** (2008), 1215, arXiv:0706.4119.
16) E. van Beveren, C. Dullemond and G. Rupp, Phys. Rev. D **21** (1980), 772, [Errata; **22** (1980), 787].
17) E. van Beveren, G. Rupp, T. A. Rijken and C. Dullemond, Phys. Rev. D **27** (1983), 1527.
18) E. van Beveren, C. Dullemond and T. A. Rijken, Z. Phys. C **19** (1983), 275.
19) A. G. Verschuren, C. Dullemond and E. van Beveren, Phys. Rev. D **44** (1991), 2803.
20) J. R. Peláez, J. Nebreda and G. Rios, arXiv:1007.3461.
21) E. Eichten, *In *Cargese 1975, Proceedings, Weak and Electromagnetic Interactions At High Energies, Part A*, New York 1976, 305–328.*
22) N. A. Törnqvist, Annals Phys. **123** (1979), 1.
23) N. A. Törnqvist, Phys. Rev. Lett. **49** (1982), 624.
24) K. Heikkilä, S. Ono and N. A. Törnqvist, Phys. Rev. D **29** (1984), 110, [Errata; **29** (1984), 2136].
25) E. van Beveren, Z. Phys. C **21** (1984), 291, hep-ph/0602246.
26) E. van Beveren and G. Rupp, Eur. Phys. J. C **22** (2001), 493, hep-ex/0106077.
27) E. van Beveren and G. Rupp, Annals Phys. **324** (2009), 1620, arXiv:0809.1149.
28) E. van Beveren, X. Liu, R. Coimbra and G. Rupp, Europhys. Lett. **85** (2009), 61002, arXiv:0809.1151.
29) S. Coito, G. Rupp and E. van Beveren, arXiv:1005.2486.
30) G. Rupp, S. Coito and E. van Beveren, arXiv:1005.2490.
31) S. Coito, G. Rupp and E. van Beveren, Phys. Rev. D **80** (2009), 094011, arXiv:0909.0051.
32) S. Coito, G. Rupp and E. van Beveren, arXiv:0812.1527.
33) E. van Beveren and G. Rupp, Phys. Rev. D **80** (2009), 074001, arXiv:0908.0242.
34) E. van Beveren, T. A. Rijken, K. Metzger, C. Dullemond, G. Rupp and J. E. Ribeiro, Z. Phys. C **30** (1986), 615, arXiv:0710.4067.
35) J. A. Oller and E. Oset, Phys. Rev. D **60** (1999), 074023, hep-ph/9809337.
36) J. A. Oller, E. Oset and J. R. Peláez, Phys. Rev. D **59** (1999), 074001, [Errata; **60** (1999), 099906], hep-ph/9804209.
37) D. R. Boito, P. C. Magalhães, M. R. Robilotta and G. R. S. Zarnauskas, AIP Conf. Proc. **1030** (2009), 340. arXiv:0805.0552.
38) D. R. Boito, P. C. Magalhães, M. R. Robilotta and G. R. S. Zarnauskas, arXiv:0805.4803.
39) R. Molina and E. Oset, Phys. Rev. D **80** (2009), 114013, arXiv:0907.3043.
40) D. Gamermann, E. Oset, D. Strottman and M. J. Vicente Vacas, Phys. Rev. D **76** (2007), 074016, hep-ph/0612179.
41) L. Roca and E. Oset, Phys. Rev. D **82** (2010), 054013, arXiv:1005.0283.
42) A. Martinez Torres, K. P. Khemchandani and E. Oset, Phys. Rev. C **77** (2008), 042203, arXiv:0706.2330.
43) K. P. Khemchandani, A. Martinez Torres and E. Oset, Eur. Phys. J. A **37** (2008), 233, arXiv:0804.4670.
44) J. R. Peláez, C. Hanhart, J. Nebreda and G. Rios, arXiv:1003.0364.
45) A. M. Torres, K. P. Khemchandani, D. Gamermann and E. Oset, Phys. Rev. D **80** (2009), 094012, arXiv:0906.5333.
46) A. Martinez Torres, K. P. Khemchandani and E. Oset, Phys. Rev. C **79** (2009), 065207, arXiv:0812.2235.
47) C. E. Jimenez-Tejero, A. Ramos and I. Vidana, Phys. Rev. C **80** (2009), 055206, arXiv:0907.5316.
48) E. van Beveren and G. Rupp, arXiv:0904.4351.
49) E. van Beveren and G. Rupp, arXiv:0906.2278.
50) E. van Beveren and G. Rupp, arXiv:1005.3490.

51) E. van Beveren and G. Rupp, Int. J. Theor. Phys. Group Theor. Nonlin. Opt. **11** (2006), 179, hep-ph/0304105.
52) E. van Beveren and G. Rupp, Phys. Rev. Lett. **91** (2003), 012003, hep-ph/0305035.
53) E. Oset *et al.*, arXiv:1008.0466.
54) J. R. Taylor, *Scattering Theory: The quantum theory on nonrelativistic collisions*, John Wiley and Sons, Inc., New York (1972).
55) E. van Beveren, T. A. Rijken, C. Dullemond and G. Rupp, Lect. Notes Phys. **211** (1984), 331.